Determination of carrier density in Te-doped Bi nanowires

Yu-Ming Lin[a] and M. S. Dresselhaus[a),b),c)]
Massachusetts Institute of Technology, Cambridge, Massachusetts 02139-4307

(Received 12 May 2003; accepted 29 July 2003)

A promising approach is presented to characterize the carrier density in Te-doped Bi nanowires from their temperature-dependent resistance measurements. This method is based on the comparison of the scattering rates due to charged impurity scattering and due to other scattering mechanisms that are independent of the carrier density. The result shows that the Te doping efficiency δ_e is only about 10%–15% for Te-doped Bi nanowires synthesized in an alumina template by molten-metal pressure injection. This analysis technique can be extended to other nanowire systems to provide valuable information regarding the carrier concentration and the Fermi energy for use in controlling and optimizing properties for specific applications. © *2003 American Institute of Physics.*
[DOI: 10.1063/1.1614443]

Studies on nanostructured materials have attracted significant attention because of their properties that are absent in bulk materials and their potential for various applications. Recent advances in materials science and microfabrication techniques,[1–4] have made it possible to fabricate various interesting nanostructures. Nanowires are especially important because they are candidates for interconnects and could also be used as active components in nanoscale electronic[5] and photonic devices.[6] Although the materials properties of nanowires have been extensively studied and various techniques have been developed to manipulate their geometrical configurations,[7] their electrical properties, however, have thus far been less investigated. Few techniques are presently available to control the fundamental electrical attributes of nanowires, mainly due to the challenges in performing transport measurements on nanowires[8] and in interpreting experimental results.

The carrier density and the Fermi energy (E_F) are important fundamental parameters for determining the electrical transport properties of nanowires and for optimizing their performance for certain applications, such as thermoelectrics. The proper placement of E_F is essential to take advantage of the unique ID band structure and density of states of nanowires. Conventional techniques used to obtain E_F or the carrier concentration in bulk crystalline materials include measurements of the Hall effect, the Shubnikov–de Haas (SdH) and related effects in a magnetic field, and the plasma frequency. Due to the quasi-1D nature of nanowires, the Hall measurement, which is basically a 2D phenomenon, may not be applicable to nanowire systems. SdH oscillations as a function of magnetic field applied parallel to the nanowire axis could, in principle, provide the most direct measurement of E_F and the carrier density. Although SdH oscillations have been reported for Bi nanowire samples with a rather large wire diameter ($\sim$200 nm),[9] the SdH measurements may not be practical for smaller diameter ($\leqslant$100 nm) or highly doped nanowires. First, in order to confine the cyclotron orbits within the small nanowire cross section, a large magnetic field is required, which may cause the first Landau level to rise above the Fermi energy and no further oscillation would be observed. Second, for highly doped nanowires, the charged impurity scattering due to the dopant atoms would decrease the electron mean free path significantly, thus preventing the formation of well-defined Landau levels. The plasma frequency in optical measurements is often employed to determine the carrier concentration and E_F in metals. However, the interpretation of optical measurements on nanowires must be carefully made, because the wire diameter is generally much smaller than the wavelength of the incident light, and the results may also depend on the light polarization relative to the wire axis.[10,11] Recently, effort has also been made to derive the carrier concentration in a single nanowire from electrical conductivity measurements.[8] In these measurements, the surface condition and contact problems become important issues, which must be overcome and addressed in order to obtain useful information.

Seebeck coefficient (S) measurements offer a promising tool to characterize E_F, because of the sensitive dependence of S on E_F. In addition, since Seebeck measurements are independent of the number of nanowires contributing to the signal, such measurements on an array of uniform diameter nanowires should be as informative as single-wire measurements. Based on the Seebeck measurements on $Bi_{1-x}Sb_x$ nanowire arrays[12] the carriers due to uncontrolled impurities in undoped nanowires were found to be n type and with carrier concentrations $\sim 1\times10^{16}$–4×10^{16} cm^{-3}. By using the SdH oscillations in magnetoresistance,[9] along with Seebeck measurements, Heremans *et al.* have reported higher carrier concentrations of $\sim 10^{17}$ cm^{-3} due to uncontrolled impurities in their Bi nanowires that were synthesized by vapor deposition.

Due to limited experimental methods available for measuring nanowire properties, theoretical modeling plays an important role in deriving the Fermi energy from accessible transport measurements. In this letter we report an approach to determine the carrier density and E_F of Te-doped Bi nanowires with a wire diameter of 40 nm by comparing the temperature dependence of experimentally derived carrier mobility with that of calculated results.

Bismuth (Bi) is an attractive material for transport stud-

[a)]Department of Electrical Engineering and Computer Science.
[b)]Department of Physics.
[c)]Electronic mail: millie@mgm.mit.edu

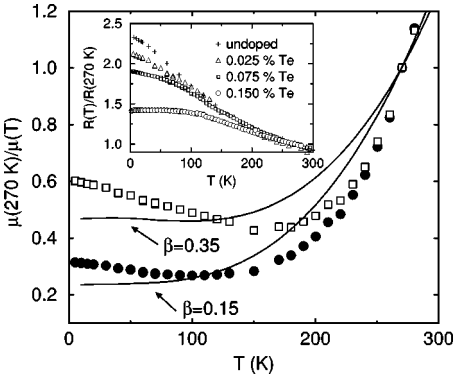

FIG. 1. Temperature dependence of $\mu_{\text{eff}}^{-1}(T)$ for 40-nm-Te-doped Bi nanowires with a nominal Te concentration of 0.025 at. %. The data points represent the normalized carrier mobility $\mu_{\text{eff}}(270\ \text{K})/\mu_{\text{eff}}(T)$ calculated for two different dopant efficiencies, $\delta_e = 0.1$ (●) and 0.2 (□), which correspond to N_d values of 6.67×10^{17} and $1.34\times10^{18}\ \text{cm}^{-3}$, respectively. The solid curves are fitting curves. Inset: measured $R(T)/R(270\ \text{K})$ for 40-nm-undoped and Te-doped-Bi nanowires with different Te dopant concentrations (Ref. 13).

ies in low-dimensional systems. Bi-related nanowires have been predicted to be promising thermoelectric materials with enhanced efficiency that may be of practical interest.[13,14] Since Te atoms serve as a *n*-type dopant in Bi, the carrier density is related to the density of ionized Te atoms, which also contribute to the charged impurity scattering processes. Therefore, by comparing the strength of the ionized impurity scattering to the other scattering mechanisms that are independent of the density of ionized impurities, the carrier density in the nanowires could be obtained. Knowledge of the actual carrier concentration in nanowires can provide guidance to control the Fermi energy during the synthesis process, which is essential for nanowire-based applications to take advantage of the unique 1D density of states in order to achieve desired functionality and optimal thermoelectric performance.

The temperature-dependent resistance $R(T)$ of Te-doped Bi nanowire arrays has been measured and reported previously,[13] as shown in the inset of Fig. 1 for the normalized resistance $R(T)/R(270\ \text{K})$ of 40-nm-Bi nanowires with various Te dopant concentrations (0.0, 0.025, 0.075, and 0.150 at. %). These Te-doped Bi nanowires were synthesized by pressure injecting molten metal alloys into the nanochannels of anodic alumina,[13] and they possess a preferred $[01\bar{1}2]$ crystal growth direction along the wire axis and a narrow diameter distribution ($\leqslant$10% variation) along the entire wire length ($\sim$50 μm) and between different nanowires in the template.[13] Since the freezeout temperature of Te atoms in 40-nm-Bi nanowires is about 2 K,[13] we assume that all the donor atoms are ionized in our 40-nm-Bi nanowires for the temperatures of interest (4–300 K). The Te concentrations quoted here denote the atomic ratio of Bi and Te that was introduced to form the alloy prior to the nanowire synthesis. The actual Te content in the nanowires may be lower and may deviate significantly from the nominal value due to the alloy inhomogeneity and the likely segregation of Te atoms to the wire boundary during alloy solidification. One of the objectives of this letter is to determine the actual Te donor concentration N_d in the nanowires and the doping efficiency δ_e, defined as the ratio between N_d and the nominal Te concentration. The doping efficiency, which depends on the nominal Te concentration and the fabrication procedures, suggests the amount of Te that should be introduced into the metal alloy for achieving the desired carrier density in the final nanowire products.

The resistance of Te-doped Bi nanowires is determined by two competing factors: the total carrier density $n(T)$ that increases with T, and the carrier mobility that generally decreases with T. The total carriers concentration includes the highly T-dependent intrinsic carriers and the extrinsic carrier concentration N_d due to the Te donors, which is relatively T independent above the freezeout temperature. The T dependence of the resistance of Te-doped Bi nanowires weakens as the doping concentration increases (see inset of Fig. 1) because of the increasing dominance of extrinsic carriers relative to the intrinsic carriers. Compared to undoped Bi nanowires, the carriers in Te-doped samples may experience extra scattering processes due to ionized impurity scattering and to the expected higher level of dopant-induced defects and strain fields. The effect of these additional scattering mechanisms on the average carrier mobility μ_{doped} of Te-doped Bi nanowires is taken into account in accordance with Matthiessen's rule by

$$\mu_{\text{doped}}^{-1}(T) = \mu_{\text{undoped}}^{-1}(T) + \mu_{\text{imp}}^{-1}(T) + \mu_{\text{defect}}^{-1}, \tag{1}$$

where μ_{undoped} is the average mobility of the undoped Bi nanowires of the same diameter, and μ_{imp}^{-1} and μ_{defect}^{-1} are associated with the increased scattering due to ionized impurities and to lattice defects in Te-doped Bi nanowires, respectively. For undoped Bi nanowires, the average mobility is found to follow a $\mu_{\text{undoped}} \sim T^{-2.9}$ dependence[13] for $T > 100$ K due to the predominant electron–phonon scattering at high T. μ_{phonon} of Bi has a stronger T dependence than is usually observed for most materials[15] because of the T-dependent effective mass m^* of Bi that increases with increasing T.[16] The term μ_{defect}^{-1} that includes neutral impurity scattering is essentially T independent, while μ_{imp}^{-1} generally increases with decreasing T. By considering the T-dependent band structure and nonparabolic effects for electrons in Bi, an expression for μ_{doped}^{-1} in Bi nanowires has been derived as[13]

$$\mu_{\text{doped}}^{-1} \simeq a T^{2.9} + b\,\eta(T), \tag{2}$$

where

$$\eta(T) \simeq m^*(T)^{1/2} E_{gL}(T)^{-2/3}, \tag{3}$$

is an approximate T dependence of $\mu_{\text{imp}}^{-1} + \mu_{\text{defect}}^{-1}$ and $E_{gL}(T)$ is the direct band gap between the L-point conduction and valence bands in bulk Bi. Although values of both a and b are required to estimate the absolute values of $\mu_{\text{doped}}(T)$ [see Eq. (2)], the T dependence of $\mu_{\text{doped}}(T)$ (or the normalized mobility $\mu_{\text{doped}}(270\ \text{K})/\mu_{\text{doped}}(T)$, as will be discussed below) only depends on the ratio of a and b. The ratio β, defined as $\beta \equiv b/a$, expresses the importance of ionized impurity scattering relative to electron–phonon scattering. a and b (and thus β) are expected to depend on the materials properties of nanowires, such as the crystallographic orientation, the wire diameter, and the donor concentration. However, since the nanowires studied here all possess the same $[01\bar{1}2]$ crystallographic direction along the wire axis and a

circular cross section with a diameter of 40 nm, the major factor that affects β for different Te-doped nanowire samples is the Te donor concentration. Since the charged impurity scattering rate, or $b\eta(T)$, is proportional to N_d whereas the term $\mu_{\text{undoped}}^{-1}=aT^{2.9}$ is expected to be the same for these Te-doped Bi nanowires, the ratio β should be approximately proportional to N_d, and this relation may be useful to determine the carrier concentration N_d.

In the following, we employ the measured $R(T)/R(270\ \text{K})$ and the calculated carrier density $n(T)$ of Te-doped Bi nanowires to obtain a correlation between β and N_d. For a measured $R(T)/R(270\ \text{K})$ curve and an assumed Te donor concentration N_d, the normalized effective carrier mobility $\mu_{\text{eff}}(T)/\mu_{\text{eff}}(270\ \text{K})$ is first obtained using the relation $\sigma(T)=en(T)\mu_{\text{eff}}(T)$, where $n(T)$ is the total carrier concentration calculated based on the model developed for Bi-related nanowires.[14] The calculation of $n(T)$ takes into account the quantized subbands formed within nanowires, the T-dependent anisotropic band structure parameters of Bi, and the $[01\bar{1}2]$ crystallographic orientation along the wire axis observed in these nanowires. The β value, associated with the assumed N_d, can then be obtained by fitting Eq. (2) with the carrier mobility $\mu_{\text{eff}}(T)$ derived experimentally. For example, Fig. 1 shows the T dependence of the normalized carrier mobility of 0.025 at. % Te-doped Bi nanowires (40 nm diameter) assuming two different N_d values: $6.67\times10^{17}\ \text{cm}^{-3}$ (filled circles) and $1.33\times10^{18}\ \text{cm}^{-3}$ (clear squares), which correspond to doping efficiencies δ_e of 0.1 and 0.2, respectively. For 0.025 at. % Te-doped Bi nanowires, each set of mobility data points of different doping efficiencies ($\delta_e=0.1$ and 0.2) can be fitted by Eq. (2) with $\beta=0.15$ and 0.35 (see solid curves in Fig. 1), respectively. The minimum in the data points of $\mu_{\text{eff}}(T)/\mu_{\text{eff}}(270\ \text{K})$ of Te-doped Bi nanowires (see Fig. 1), also observed in the modeled $\mu_{\text{eff}}(T)/\mu_{\text{eff}}(270\ \text{K})$ curves for larger β values, is due to the ionized impurity scattering with a scattering rate τ_{imp}^{-1} that increases with decreasing T. The discrepancy between the data points and the fitting curves (see Fig. 1) could be due to a poorly assumed N_d value compared to the actual Te donor concentration or factors not considered in our model such as the electron–electron scattering, which may be important at low temperatures and high carrier concentrations, and energy-dependent scattering times for τ_{imp} and τ_{undoped}. Nevertheless, a reasonable fitting can be obtained for the two donor concentrations assumed in Fig. 1, indicating that the actual carrier concentration N_d cannot be uniquely determined for this Te-doped Bi nanowire sample, and additional information and further analysis are required, as illustrated below.

By applying the mobility fitting procedures to other Te-doped nanowires assuming various doping efficiencies ($\delta_e=0.1$,0.2, 0.3, etc.), Fig. 2 shows the calculated β values as a function of N_d for three Te-doped Bi nanowire samples with nominal Te concentrations of 0.025 at. % (clear circles), 0.075 at. % (clear squares), and 0.15 at. % (clear diamonds). These data points form possible combinations of β-N_d pairs for each nanowire sample according to the mobility fitting mentioned above. We should note that the multiple β-N_d pairs derived for each sample [e.g., the six data points represented by (clear circles)] do not necessarily follow a linear relation since only the pair that has the *actual* donor concentration reflects the real nanowires we measured and is physically meaningful, while the other β-N_d pairs will be eliminated by further considerations (see the discussion below). We also note that for large δ_e values, there are no solutions that provide a satisfactory fit between the measured mobility and Eq. (2), and the upper limits of δ_e are found to be 0.6, 0.3, and 0.2 for 0.025, 0.075, and 0.150 at. % Te-doped Bi nanowires, respectively. In order to determine the β-N_d pairs that correspond to the actual samples, we utilize the expected linear dependence between β and N_d. An empirical relation between β and N_d, which satisfies this linear condition and passes through certain β-N_d pairs for all three Te-doped Bi nanowire samples is found and given by $\beta=2.48\times10^{-18}N_d$, where N_d is in units of cm^{-3} (see the dashed line in Fig. 2). According to this relation, N_d are estimated to be $\sim1.00\times10^{18}$, 2.00×10^{18}, and $4.00\times10^{18}\ \text{cm}^{-3}$ for 0.025, 0.075, and 0.15 at. % Te-doped Bi nanowires (see Fig. 2), respectively. Since the intrinsic carrier concentration of 40-nm-Bi nanowires is only $\sim8.2\times10^{16}\ \text{cm}^3$ at 77 K,[14] we see that the total carrier concentration of these Te-doped Bi nanowires is dominated by the extrinsic carriers N_d contributed by the Te dopants. The doping efficiency δ_e is found to be ~0.10 for both 0.075 and 0.150 at. % Te-doped Bi nanowires, and $\delta_e\sim0.15$ for 0.025 at. % Te-doped Bi nanowires, indicating that in nanowires fabricated in anodic alumina templates by the pressure injection technique, δ_e increases somewhat with decreasing nominal Te dopant concentration. We note that this empirical relation is of great significance since it provides a universal calibration curve to determine the Te donor concentration in Bi nanowires using $R(T)$ measurements.

With N_d in the nanowires thus obtained, the Fermi energies at 77 K are calculated to be ~62, 78, and 97 meV for 0.025, 0.075, and 0.15 at. % Te-doped Bi nanowires, respectively, where the zero in energy refers to the L-point conduction band edge in bulk Bi. The inset to Fig. 2 shows the calculated density of states as a function of energy for 40-

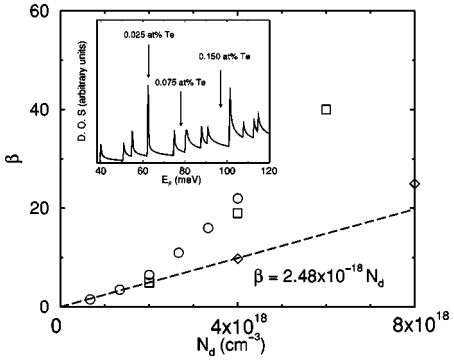

FIG. 2. Calculated β values as a function of donor carrier concentration N_d for three Te-doped Bi nanowires with nominal Te concentrations of 0.025 at. % (○), 0.075 at. % (□), and 0.150 at. % (◇). The various data points of each nanowire sample denote the calculated β values assuming different doping efficiencies ($\delta_e=0.1$, 0.2, 0.3, etc.). The dashed line shows the empirical relation derived for β and N_d for actual Bi nanowires measured in this work. Inset: calculated density of states as a function of energy for 40-nm-Bi nanowires (oriented in the $[01\bar{1}2]$ direction) at 77 K. The zero in energy refers to the L-point conduction band edge in bulk Bi. The arrows indicate the Fermi energies of 0.025, 0.075, and 0.150 at. % Te-doped Bi nanowires at $E_F\sim62$, 78, and 97 meV, respectively.

nm-Bi nanowires (oriented in the $[01\bar{1}2]$ direction) at 77 K, and the Fermi energies of the three Te-doped Bi nanowires are indicated by the arrows. The density of states here is calculated using the theoretical model developed for Bi nanowires,[14] taking into account the anisotropic and multiple carrier pockets and the cylindrical wire boundaries. For thermoelectric applications, the optimal Fermi energy for 40-nm-Bi nanowires oriented in the $[01\bar{1}2]$ direction is predicted[14] to be ~ 87 meV, which can be achieved with a donor concentration N_d of $\sim 2.73\times 10^{18}$ cm^{-3}. Therefore, a 0.10 at. % Te-doped Bi alloy should be used when preparing nanowires by pressure injection, assuming a doping efficiency of ~ 0.1, in order to achieve this optimal carrier concentration for thermoelectric applications.

In summary, we present here a promising analytical approach to characterize the carrier density in Te-doped Bi nanowires from measurements on their $R(T)$. Unlike techniques conventionally employed for characterizing bulk materials, the present method is based on the comparison of the scattering rates due to the ionized impurity scattering and other scattering mechanisms that are independent of the carrier density. The result shows that the Te doping efficiency δ_e in Bi nanowires is only about 10%–15% for nanowires synthesized in anodic alumina templates by molten-metal pressure injection, and δ_e decreases slightly as the Te content in the bulk alloy increases. The results not only provide valuable information regarding the carrier concentration and the Fermi energy, but also offer practical guidance to control and optimize these important parameters during nanowire synthesis for specific applications based on nanowires. Furthermore, the analysis approach developed here can also be extended to other nanowire systems to examine these fundamental electrical properties.

The authors thank O. Rabin, S. B. Cronin, G. Dresselhaus, J. J. Ying, G. Chen, and J. Heremans for valuable discussions. The support from ONR Grant Nos. N00014-02-1-0865 and NSF DMR-01-16042 is gratefully acknowledged.

[1] Y. Wu and P. Yang, J. Am. Chem. Soc. **123**, 3165 (2001).
[2] N. A. Nelosh, A. Boukai, F. Diana, B. Geradot, A. Badolato, P. M. Petroff, and J. R. Heath, Science **300**, 112 (2003).
[3] Z. Zhang, J. Y. Ying, and M. S. Dresselhaus, J. Mater. Res. **13**, 1745 (1998).
[4] C. B. Murray, C. R. Kagan, and M. G. Bawendi, Science **270**, 1335 (1995).
[5] Y. Huang, X. F. Duan, Y. Cui, L. J. Lauhon, K.-H. Kim, and C. M. Lieber, Science **294**, 1313 (2001).
[6] M. H. Huang, S. Mao, H. Feick, H. Yan, Y. Wu, H. Kind, E. Weber, R. Russo, and P. Yang, Science **292**, 1897 (2001).
[7] Y. Xia, P. Yang, Y. Sun, Y. Wu, B. Mayers, B. Gates, Y. Yin, F. Kim, and H. Yan, Adv. Mater. (Weinheim, Ger.) **15**, 353 (2003).
[8] S. B. Cronin, Y.-M. Lin, O. Rabin, M. R. Black, J. Y. Ying, M. S. Dresselhaus, P. L. Gai, J.-P. Minet, and J.-P. Issi, Nanotechnology **13**, 653 (2002).
[9] J. Heremans and C. M. Thrush, Phys. Rev. B **59**, 12579 (1999).
[10] M. R. Black, M. Padi, S. B. Cronin, Y.-M. Lin, O. Rabin, T. McClure, G. Dresselhaus, P. L. Hagelstein, and M. S. Dresselhaus, Appl. Phys. Lett. **77**, 4142 (2000).
[11] M. R. Black, Y.-M. Lin, S. B. Cronin, O. Rabin, and M. S. Dresselhaus, Phys. Rev. B **65**, 195417 (2002).
[12] Y.-M. Lin, O. Rabin, S. B. Cronin, J. Y. Ying, and M. S. Dresselhaus, Appl. Phys. Lett. **81**, 2403 (2002).
[13] Y.-M. Lin, S. B. Cronin, J. Y. Ying, M. S. Dresselhaus, and J. P. Heremans, Appl. Phys. Lett. **76**, 3944 (2000).
[14] Y.-M. Lin, X. Sun, and M. S. Dresselhaus, Phys. Rev. B **62**, 4610 (2000).
[15] H. Brooks, Adv. Electron. Electron Phys. **7**, 158 (1955).
[16] M. P. Vecchi and M. S. Dresselhaus, Phys. Rev. B **10**, 771 (1974).